Patrick Grosch
Institut de Robòtica i Informàtica Industrial (CSIC-UPC)
Llorens Artigas 4-6, 2 planta
08028 Barcelona – Spain
E-mail: pgrosch@iri.upc.edu

Raffaele Di Gregorio
Department of Engineering
University of Ferrara
Via Saragat, 1
44100 FERRARA - Italy
raffaele.digregorio@unife.it

Federico Thomas
Institut de Robòtica i Informàtica Industrial (CSIC-UPC)
Llorens Artigas 4-6, 2 planta
08028 Barcelona – Spain
E-mail: fthomas@iri.upc.edu

Generation of Under-Actuated Manipulators with Non-Holonomic Joints from Ordinary Manipulators

This paper shows how to generate under-actuated manipulators by substituting non-holonomic spherical pairs (nS pairs) for (holonomic) spherical pairs (S pairs) in ordinary (i.e. not under-actuated) manipulators. As a case study, an under-actuated manipulator, previously proposed by one of the authors, is demonstrated to be generated, through this pair substitution, from an inversion of the 6-3 fully-parallel manipulator (FPM). Moreover, the kinetostatic analysis of this under-actuated manipulator is reconsidered, and a simple and compact formulation is obtained. The results of this kinetostatic analysis can be used both in the design of the under-actuated manipulator, and in its control.
Keywords: *kinetostatics, non-holonomic constraint, ordinary manipulator, under-actuated manipulator, parallel manipulator.*

NOMENCLATURE

P = prismatic pair
U = universal joint
S = spherical pair
nS = non-holonomic spherical pair
SPU = spherical-prismatic-universal kinematic chain (limb)
nSPU = (non-holonomic spherical)-prismatic-universal kinematic chain (limb)
FPM = fully parallel manipulator
DPA = direct position analysis
dof = degrees-of-freedom
RB = rigid body

1 Introduction

Non-holonomic constraints arise in many different areas of robotics [1-4] such as motion planning and control of mobile robots, reorientation of free-flying space robots, rolling contacts of multi-fingered hands, etc. In all these cases, the non-holonomic constraints are inherent to the problem, but there are some cases in which the artificial introduction of this kind of constraints can provide important advantages.

In pick-and-place applications of manipulators, only the initial and the final poses (position and orientation) of the end effector are assigned by the task, whereas the end-effector path between them is free. The ideal manipulator for these applications should be able to make the end effector reach any pose in the six-dimensional operational space, and, by exploiting the free fly of the end effector, it should be able to satisfy additional design conditions that reduce its hardware complexity. Joints with non-holonomic constraints do not reduce the reachable relative poses of the links connected by the joint since non-holonomic constraints have the only effect of reducing the set of paths that can be covered for moving between two reachable relative poses. This reduction of practicable paths is accompanied by the rising of new reaction forces in the joint which can be usefully exploited to eliminate actuators. Thus, designing a manipulator with fewer actuators than the degrees-of-freedom (dof)[1] of its configuration space ---to reduce bulk, weight and expense--- becomes feasible by introducing mechanical elements that lead to non-holonomic constraints.

The literature on the use of non-holonomic devices in the design of manipulators is limited to few examples. In [7], Stammers et al. presents a robot wrist that can attain any orientation with two motors only. This is achieved by means of a friction drive, using rollers on a spherical ball to which the end effector is fixed, and by fixing the two motors to the arm. In [8], Peshkin et al. present a passive spherical robot which can display programmable constraints. The device is based on a non-holonomic element involving a sphere and three reorientable rollers. In [9], Nakamura et al. describe an n-joint serial robot which can reach any pose in its n-dimensional configuration space with only two actuators. The joints of this manipulator are coupled by (n-1) non-holonomic devices, based on spheres and rollers, so that it reaches a desired pose by following a path whose computation is algorithmically equivalent to maneuvering a car with n-trailers. More recently, in [10], Ben-Horin and Thomas proposed a three-legged parallel robot where each leg is connected to the base through a sphere whose motion is constrained by a roller. This latter parallel architecture permits to attain any

[1] The degrees-of-freedom (dof) of the configuration space, also called configuration (or finite) dof [5], are the minimum number of geometric parameters necessary to uniquely identify the configuration of the mechanical system [6]. They may be different from the instantaneous dof, also called velocity dof [5], of the same mechanical system.

position and orientation for the platform using only three prismatic actuators.

Despite the difference of purpose, all mentioned examples include at least one sphere whose motion is constrained by a roller that can freely roll in contact with the sphere without slipping laterally. This no-slip constraint is a non-holonomic constraint, a constraint relating the velocities of the sphere and the roller. The kinematics of this sphere-roller assembly is equivalent to that of a unicycle on a sphere whose equations of motion can be represented by first-order differential equations [11].

Many research efforts have been made to clarify different aspects of non-holonomic mechanical systems including its controllability, stability, feedback stabilization, time-periodic control, chained form transformation, etc. but, in any case, achieving a formulation for the kinematics of the system, as compact and simple as possible, is essential to explore the applicability of all these results available in the literature.

Herein, how under-actuated manipulators can be generated through the substitution of a spherical pair (S pair) by a particular non-holonomic pair, named non-holonomic spherical pair (nS pair), in ordinary (i.e., not under-actuated) manipulators is shown. As a case study, the under-actuated parallel architecture presented in [10] is demonstrated to be generable from an inversion of the 6-3 fully-parallel manipulator (FPM). Its kinetostatic analysis is reformulated, and a simple and compact formulation, useful for its design and control, is obtained.

This paper is structured as follows. Next section describes how to generate under-actuated manipulators through substitution of suitable kinematic pairs in ordinary manipulators. Section 3 is devoted to the case study: a compact formulation for its instantaneous kinematics and statics is obtained, and some clues for the characterization of its singularities are provided. Eventually, section 4 offers the conclusions.

2 Generation of Under-Actuated Manipulators

Two rigid bodies (RBs) connected by a spherical pair (S pair) can assume any relative orientation, and can move from one relative orientation to another by covering any spherical-motion path that joins the two relative orientations. Actually, the possibility of freely orientating two RBs with respect to one another is not related to the possibility of performing relative rotations around axes which pass through the center of spherical motion and have any direction. In fact, a suitable sequence (at least three) of finite rotations around coplanar axes that pass through the spherical-motion center can freely orientate one RB with respect to another. Thus, if the only free relative orientation of two RBs is required, the use of an S pair will be redundant. The use of a kinematic pair that allows only rotations around coplanar axes that pass through a fixed point would be sufficient.

Due to frictional forces, the rolling contact between a sphere and a roller forbids the sphere rotations around the axis through the sphere center, and perpendicular to the plane defined by the roller axis and the sphere center. By combining such a non-holonomic constraint with other constraints that forbid the relative translation between the sphere center and the roller axis, a non-holonomic joint will result. This joint constrains two RBs: one fixed to the sphere and the other fixed to the plane, defined by the roller axis and the sphere center. So that the resulting constrained motion permits only relative rotations around axes lying on the above-mentioned plane and passing through the sphere center. Hereafter, this type of joint will be called non-holonomic spherical pair (nS pair).

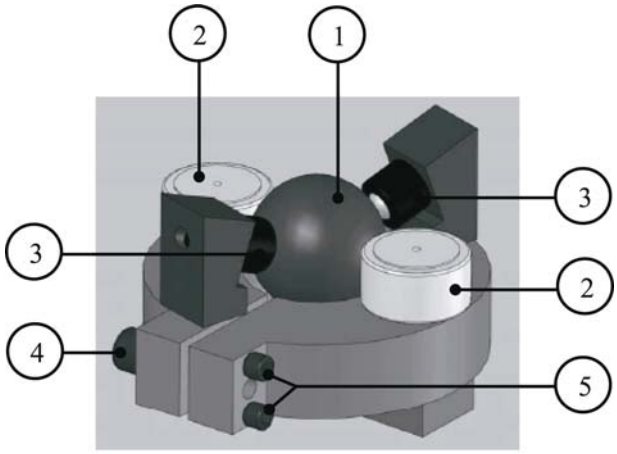

Figure 1. 3D CAD model of one out of many different manufacturing schemes for the nS pair: (1) sphere, (2) roller (carried out through a roller bearing), (3) spherical bearing [there are three spherical bearing (only two are visible) that forbids the translation of the sphere], (4) pre-load adjust screw, and (5) parallelism adjust screws.

The constraint forces, which two RBs, joined by a nS pair, exert on one another through the joint, can be reduced to a resultant force applied on the sphere center and a torque perpendicular to the plane defined by the roller axis and the sphere center. The torque is the static effect of the non-holonomic constraint, whereas the resultant force on the sphere center is the same static effect that an S pair would have generated.

An nS pair could be manufactured as shown in Fig. 1. From a manufacturing point of view, it is worth noting that, in a nS pair, the presence of any number of roller-sphere contacts does not alter the kinetostatics of the nS pair, provided that all the roller axes lie on a same plane passing through the sphere center[2]. Moreover, the maximum torque transmitted through the nS pair, due to its frictional origin, can be fixed by suitably choosing the number of roller-sphere contacts together with the normal force transmitted through each contact.

The above discussion brings to the proposition: *i)* the substitution of a number of nS pairs for as many S pairs in a kinematic chain does not change the configuration space of that chain (i.e., neither the degrees-of-freedom (dof)[3] of the configuration space nor the reachable configurations change), it only reduces the practicable paths for moving that chain from one configuration to another.

Moreover, due to the torque that arises in a nS pair and to proposition *i)*, the following proposition holds, too: *ii)* in a manipulator, the substitution of a number of nS pairs for as many S pairs does not change its workspace and allows the elimination of a number of actuators equal to the number of introduced nS pairs (i.e., generates an under-actuated manipulator).

S pairs are extensively employed in spatial parallel manipulators (see, for instance, [12-15]). In particular, fully-

[2] In general, two rollers whose axes locate with the sphere center two different planes constrains the sphere to rotate around the intersection line between the two planes, whereas three rollers whose axes locate with the sphere center three different planes lock the sphere.

[3] The presence of non-holonomic constraints does not change the configuration dof [5, 6]. It only affects the instantaneous dof of the mechanism. Hereafter, the acronym dof used alone will mean configuration dof.

parallel manipulators (FPMs) feature two platforms, one mobile (end effector) and the other fixed (frame), connected to each other by means of six universal(U)-prismatic(P)-spherical(S) kinematic chains (UPS limbs) where the prismatic pairs are the only actuated pairs. In each limb, the centers of the universal joint and of the spherical pair (limb's attachment points) are points, fixed either to the end effector or to the frame, whose distance (limb length) is controlled by the actuated prismatic pair. Two or more attachment points, either in the end effector or in the frame, can coalesce into a unique point. According to the number of attachment points (no matter if they are multiple or not) in the end effector, say p, and in the frame, say q, different FPM architectures, named p-q FPM, are distinguished [15].

Due to the high number of S pairs appearing in FPMs, the substitutions of nS pairs for S pairs, accompanied by as many eliminations of actuators in the prismatic pairs, can be operated in many ways in all the FPM architectures. By exploiting all the possible substitutions, a lot of new under-actuated parallel manipulators can be generated. It is worth noting that a passive UPS limb only affects the workspace borders since it has connectivity six, and, if this effect is not necessary, the elimination of the actuator in a prismatic pair could be accompanied by the elimination of the whole resulting passive UPS limb.

3 Case Study

In this section, an under-actuated parallel manipulator generated from the 6-3 FPM (Fig. 2) is studied.

The 6-3 FPM architecture features three couples of UPS limbs with coalesced S pairs in the end effector. This architecture was proposed first by Stewart [16], in the 1965, for a flight simulator. Successively, with the renewed interest for the parallel architectures, started at the end of the eighties, it was diffusely studied. In particular, regarding the direct position analysis of the 6-3 FPM, Innocenti and Parenti-Castelli [17] demonstrated that at most sixteen end-effector poses correspond to a given set of limb lengths. Then, Parenti-Castelli and Di Gregorio [18] demonstrated that the end-effector pose is uniquely determined when the value of one passive joint variable is measured besides the six limb lengths. The direct position analysis of this FPM can also be used for spatial parallel manipulators that become 3-RS structures when the actuators are locked (see, for instance, [19-22]).

Starting from the 6-3 architecture, each couple of UPS limbs with coalesced S pairs (Fig. 3(left)) can be transformed into an UPnS limb, as shown in Fig 3(right), without affecting the workspace of the manipulator (see proposition *i)*). By operating this substitution in all the three couples of UPS limbs together with the inversion of the end effector with the frame, the under-actuated manipulator with topology 3-nSPU, shown in Fig. 4, is obtained. This under-actuated manipulator is able to move the end effector in a six-dof workspace by changing only the three limb lengths. The 3-nSPU has been proposed first in [10].

Regarding the direct position analysis (DPA) of the 3-nSPU, since its configuration space has six dof, a number of closure equations equals to the number of unknowns can be written if, and only if, over the three limb lengths, three more passive joint variables are assigned (measured). By assigning (measuring) the three joint variables of the three revolute pairs[4] not adjacent to the end effector, the closure equation system coincides with the one of the 6-3 FPM for assigned limb lengths [18], and admits at most sixteen solution for the end-effector pose. Moreover, if the joint variable of a revolute pair adjacent to the end effector is measured (or coherently assigned) too, only one end-effector pose satisfies the closure equations [18].

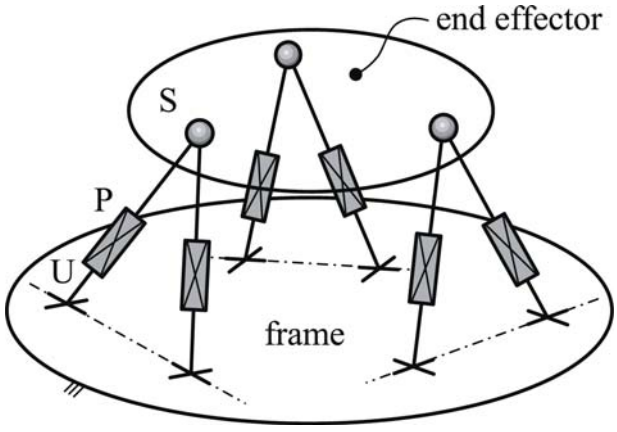

Figure 2. 6-3 FPM

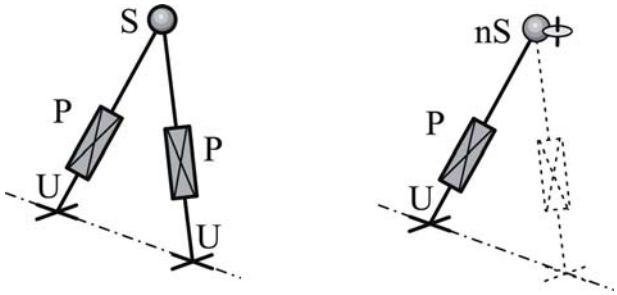

Figure 3. UPnS limb (*right*) generated by substituting an nS pair for the S pair in the two UPS limbs with coalesced S pairs (*left*).

3.1 Instantaneous Kinematics: Fig. 5 shows the i^{th} limb, i = 1, 2, 3, together with the notation that will be used. $\mathbf{w}_{1i}$ and $\mathbf{w}_{2i}$ are two any mutually orthogonal unit vectors fixed to the frame and lying on the plane defined by the roller axis and the center, A_i, of the sphere, in the roller-sphere contact. $\mathbf{w}_{3i}$ and $\mathbf{w}_{4i}$ are the two mutually orthogonal unit vectors of the axes of the two revolute pairs constituting the U joint. B_i is the center of the U joint. $\mathbf{a}_i$ and $\mathbf{b}_i$ are the two position vectors which locate the points A_i and B_i, respectively, in a generic Cartesian reference fixed to the frame, whereas $\mathbf{p}$ is the position vector of an end-effector point, P, in the same Cartesian reference. θ_{ji}, for j =1, …, 4, is a joint variable denoting a rotation angle around the joint-axis defined by $\mathbf{w}_{ji}$, for j=1, …, 4, and positive if counterclockwise with respect to $\mathbf{w}_{ji}$. The length of the i^{th} limb is equal to $\|\mathbf{b}_i - \mathbf{a}_i\|$, and it will be denoted l_i. Moreover, the limb-axis' unit vector, $\mathbf{g}_i$, and the unit vector, $\mathbf{h}_i$ ($\mathbf{r}_i$) normal to the plane located by the U-joint's revolute-pair axes (by the roller axis together with the sphere center in the nS joint) satisfy the following relationships:

$$l_i\,\mathbf{g}_i = \mathbf{b}_i - \mathbf{a}_i, \quad \mathbf{h}_i = \mathbf{w}_{3i} \times \mathbf{w}_{4i}, \quad \mathbf{r}_i = \mathbf{w}_{1i} \times \mathbf{w}_{2i}. \tag{1}$$

The time differentiation of the first of the relationships (1) yields

[4] Each U joint is constituted by two revolute pairs: one adjacent to, and the other not adjacent to the end effector.

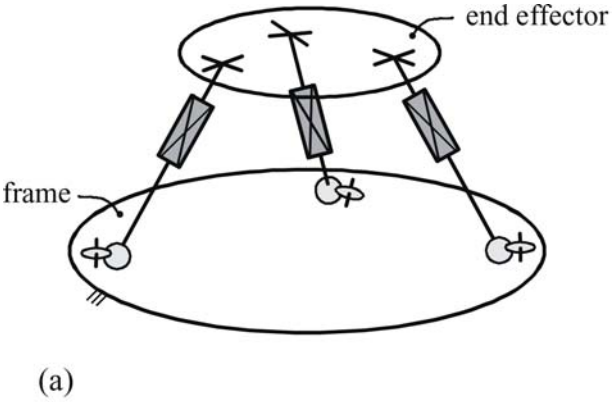

(a)

(b)

Figure 4. Under-actuated manipulator with topology 3-nSPU: (a) kinematic model, (b) 3D CAD model of a manufacturing scheme.

$$\dot{l}_i\,\mathbf{g}_i + l_i\,\dot{\mathbf{g}}_i = \dot{\mathbf{b}}_i \tag{2}$$

Since $\dot{\mathbf{g}}_i = (\dot{\theta}_{1i}\mathbf{w}_{1i} + \dot{\theta}_{2i}\mathbf{w}_{2i})\times\mathbf{g}_i$, and $\dot{\mathbf{b}}_i = \dot{\mathbf{p}} + \boldsymbol{\omega}\times(\mathbf{b}_i - \mathbf{p})$, where $\boldsymbol{\omega}$ denotes the end-effector angular velocity, Eq. (2) can be rewritten as

$$\dot{l}_i\,\mathbf{g}_i + l_i[\dot{\theta}_{1i}(\mathbf{w}_{1i}\times\mathbf{g}_i) + \dot{\theta}_{2i}(\mathbf{w}_{2i}\times\mathbf{g}_i)] = \dot{\mathbf{p}} + \boldsymbol{\omega}\times(\mathbf{b}_i - \mathbf{p}). \tag{3}$$

The dot products of (3) by $\mathbf{w}_{1i}$ and $\mathbf{w}_{2i}$ yield the following two scalar equations:

$$\dot{l}_i(\mathbf{g}_i\cdot\mathbf{w}_{1i}) + l_i\dot{\theta}_{2i}(\mathbf{w}_{2i}\times\mathbf{g}_i\cdot\mathbf{w}_{1i}) = \dot{\mathbf{p}}\cdot\mathbf{w}_{1i} + \boldsymbol{\omega}\times(\mathbf{b}_i - \mathbf{p})\cdot\mathbf{w}_{1i}, \tag{4}$$

$$\dot{l}_i(\mathbf{g}_i\cdot\mathbf{w}_{2i}) + l_i\dot{\theta}_{1i}(\mathbf{w}_{1i}\times\mathbf{g}_i\cdot\mathbf{w}_{2i}) = \dot{\mathbf{p}}\cdot\mathbf{w}_{2i} + \boldsymbol{\omega}\times(\mathbf{b}_i - \mathbf{p})\cdot\mathbf{w}_{2i}. \tag{5}$$

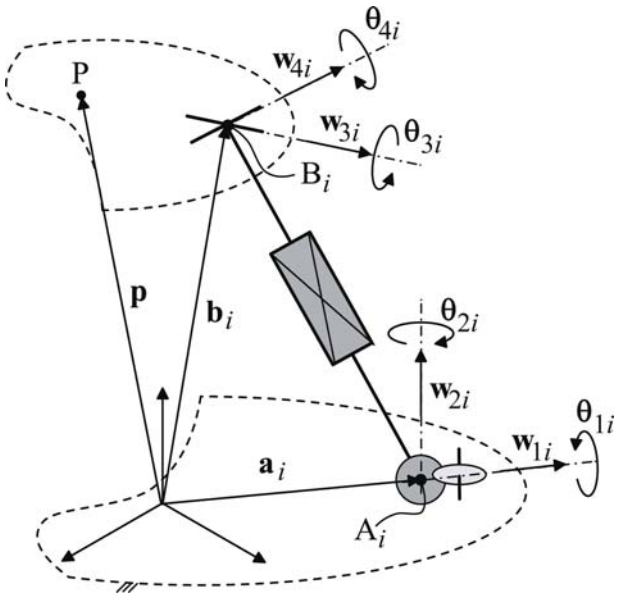

Figure 5. i^{th} limb of type nSPU: notations.

On the other hand (see Fig. 5), the end-effector angular velocity is equal to $\sum_{j=1,4}\dot{\theta}_{ji}\mathbf{w}_{ji}$, whose dot product by $\mathbf{h}_i$ gives the following expression

$$\boldsymbol{\omega}\cdot\mathbf{h}_i = \dot{\theta}_{1i}(\mathbf{w}_{1i}\cdot\mathbf{h}_i) + \dot{\theta}_{2i}(\mathbf{w}_{2i}\cdot\mathbf{h}_i).$$

Solving (4) and (5) for $\dot{\theta}_{2i}$ and $\dot{\theta}_{1i}$, respectively, and replacing the result in the above equation, yields:

$$\boldsymbol{\omega}\cdot\mathbf{h}_i = \left[\frac{\dot{\mathbf{p}}\cdot\mathbf{w}_{2i} + \boldsymbol{\omega}\times(\mathbf{b}_i - \mathbf{p})\cdot\mathbf{w}_{2i} - \dot{l}_i\mathbf{g}_i\cdot\mathbf{w}_{2i}}{l_i(\mathbf{w}_{1i}\times\mathbf{g}_i\cdot\mathbf{w}_{2i})}\right](\mathbf{w}_{1i}\cdot\mathbf{h}_i) + \left[\frac{\dot{\mathbf{p}}\cdot\mathbf{w}_{1i} + \boldsymbol{\omega}\times(\mathbf{b}_i - \mathbf{p})\cdot\mathbf{w}_{1i} - \dot{l}_i\mathbf{g}_i\cdot\mathbf{w}_{1i}}{l_i(\mathbf{w}_{2i}\times\mathbf{g}_i\cdot\mathbf{w}_{1i})}\right](\mathbf{w}_{2i}\cdot\mathbf{h}_i). \tag{6}$$

Taking into account the identities

$$\mathbf{h}_i\times\mathbf{r}_i = \mathbf{h}_i\times(\mathbf{w}_{1i}\times\mathbf{w}_{2i}) = (\mathbf{w}_{2i}\cdot\mathbf{h}_i)\mathbf{w}_{1i} - (\mathbf{w}_{1i}\cdot\mathbf{h}_i)\mathbf{w}_{2i},$$

$$\mathbf{r}_i\cdot\mathbf{g}_i = \mathbf{w}_{1i}\times\mathbf{w}_{2i}\cdot\mathbf{g}_i = -\mathbf{w}_{1i}\times\mathbf{g}_i\cdot\mathbf{w}_{2i} = \mathbf{w}_{2i}\times\mathbf{g}_i\cdot\mathbf{w}_{1i},$$

relationship (6) can be rewritten as:

$$\dot{l}_i\,\mathbf{g}_i\cdot(\mathbf{h}_i\times\mathbf{r}_i) = \dot{\mathbf{p}}\cdot(\mathbf{h}_i\times\mathbf{r}_i) + \boldsymbol{\omega}\cdot[(\mathbf{b}_i - \mathbf{p})\times(\mathbf{h}_i\times\mathbf{r}_i) - l_i(\mathbf{r}_i\cdot\mathbf{g}_i)\mathbf{h}_i]. \tag{7}$$

Since $\dot{l}_i$ can also be obtained as the projection of $\dot{\mathbf{b}}_i$ on $\mathbf{g}_i$ [see Eq. (2)], the following expression holds

$$\dot{l}_i = \dot{\mathbf{b}}_i\cdot\mathbf{g}_i = \dot{\mathbf{p}}\cdot\mathbf{g}_i + \boldsymbol{\omega}\cdot[(\mathbf{b}_i - \mathbf{p})\times\mathbf{g}_i]. \tag{8}$$

Replacing expression (8) for $\dot{l}_i$ in (7), gives

$$\dot{\mathbf{p}} \cdot \mathbf{s}_i + \boldsymbol{\omega} \cdot [(\mathbf{b}_i - \mathbf{p}) \times \mathbf{s}_i - l_i (\mathbf{r}_i \cdot \mathbf{g}_i) \mathbf{h}_i] = 0 \,. \tag{9}$$

where

$$\mathbf{s}_i = \mathbf{h}_i \times \mathbf{r}_i - [\mathbf{g}_i \cdot (\mathbf{h}_i \times \mathbf{r}_i)] \mathbf{g}_i \,. \tag{10}$$

is the component of $\mathbf{h}_i \times \mathbf{r}_i$ perpendicular to $\mathbf{g}_i$.

Eventually, rewriting Eqs. (8) and (9), for i = 1, 2, 3, in matrix form yields

$$\begin{pmatrix} \mathbf{1}_{3\times3} \\ \mathbf{0}_{3\times3} \end{pmatrix} \dot{\mathbf{i}} = \begin{pmatrix} \mathbf{G}_{3\times3} & \mathbf{K}_{3\times3} \\ \mathbf{S}_{3\times3} & \mathbf{J}_{3\times3} \end{pmatrix} \begin{pmatrix} \dot{\mathbf{p}} \\ \boldsymbol{\omega} \end{pmatrix} \tag{11}$$

where $\mathbf{1}_{3\times3}$ and $\mathbf{0}_{3\times3}$ are the 3×3 identity and zero matrix, respectively, $\dot{\mathbf{i}} = (\dot{i}_1, \dot{i}_2, \dot{i}_3)^T$ is the vector collecting the joint rates of the actuated joints, and

$$\mathbf{K}^T[i,:] = (\mathbf{b}_i - \mathbf{p}) \times \mathbf{g}_i \tag{12}$$
$$\mathbf{G}^T[i,:] = \mathbf{g}_i \tag{13}$$
$$\mathbf{J}^T[i,:] = (\mathbf{b}_i - \mathbf{p}) \times \mathbf{s}_i - l_i (\mathbf{r}_i \cdot \mathbf{g}_i) \mathbf{h}_i \tag{14}$$
$$\mathbf{S}^T[i,:] = \mathbf{s}_i \tag{15}$$

with the notation $\mathbf{A}^T[i,:]$ to mean the i-th column of matrix $\mathbf{A}^T_{3\times3}$.

Matrix relationship (11) is the sought-after input-output instantaneous relationship necessary to implement the control algorithms of the 3-nSPU.

3.2 Static Analysis: The only input-output static relationship can be immediately deduced from (11) through the principle of virtual work. Nevertheless, in order to highlight how the loads act upon the limbs and are transmitted through the joints, the complete static analysis of the 3-nSPU will be developed here independently of (11).

Figure 6 shows the free-body diagram of the i^{th} limb. With reference to Fig. 6, the force $\mathbf{f}_{bi}$ ($\mathbf{f}_{ai}$), applied on B_i (A_i), together with the torque $m_{hi}\,\mathbf{h}_i$ ($m_{ri}\,\mathbf{r}_i$) are the resultants of constraint forces exerted by the end effector (frame) on the i^{th} limb through the U joint (the nS joint). Moreover, the force $-\mathbf{f}_{ext}$, applied on the end-effector point P, together with the torque $-\mathbf{m}_{ext}$ will denote the resultants of the interaction forces exerted on the end effector. The force $\tau_i\,\mathbf{g}_i$ will denote the axial force exerted on the upper part of the i^{th} limb by the actuator in the prismatic pair. It is worth noting that the force equilibrium, along the limb axis, of the upper part of the i^{th} limb yields the following relationship $\tau_i = -\mathbf{f}_{bi} \cdot \mathbf{g}_i$.

With these notations, the equilibrium of the forces applied on the i^{th} limb yields $\mathbf{f}_{bi} + \mathbf{f}_{ai} = 0$; whereas, taking A_i as reference point, the equilibrium of the moments applied on the same limb is:

$$m_{hi}\,\mathbf{h}_i + m_{ri}\,\mathbf{r}_i + l_i\,\mathbf{g}_i \times \mathbf{f}_{bi} = \mathbf{0}. \tag{16}$$

The dot product of Eq. (16) by $\mathbf{g}_i$, yields the relationship

$$m_{ri} = -m_{hi} \frac{\mathbf{h}_i \cdot \mathbf{g}_i}{\mathbf{r}_i \cdot \mathbf{g}_i} \,. \tag{17}$$

whose substitution for m_{ri} in (16) leads to

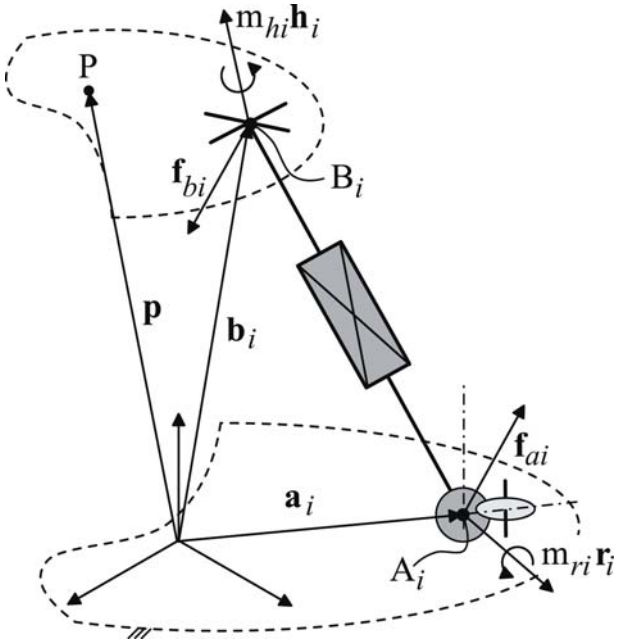

Figure 6. i^{th} **limb of type nSPU: free-body diagram.**

$$\frac{m_{hi}}{\mathbf{r}_i \cdot \mathbf{g}_i} [\mathbf{g}_i \times (\mathbf{h}_i \times \mathbf{r}_i)] + l_i\,\mathbf{g}_i \times \mathbf{f}_{bi} = \mathbf{0} \,. \tag{18}$$

where the vector identity $\mathbf{g}_i \times (\mathbf{h}_i \times \mathbf{r}_i) = (\mathbf{r}_i \cdot \mathbf{g}_i)\,\mathbf{h}_i - (\mathbf{h}_i \cdot \mathbf{g}_i)\,\mathbf{r}_i$ has been used.

The dot product of Eq. (18) by $\mathbf{h}_i \times \mathbf{r}_i$ yields the relationship: $(\mathbf{g}_i \times \mathbf{f}_{bi}) \cdot (\mathbf{h}_i \times \mathbf{r}_i) = 0$. Such a relationship is satisfied if, and only if, $\mathbf{f}_{bi}$ is a linear combination of $\mathbf{g}_i$ and $\mathbf{h}_i \times \mathbf{r}_i$. Subtracting from $\mathbf{h}_i \times \mathbf{r}_i$ its component along $\mathbf{g}_i$, the vector $\mathbf{s}_i$ is obtained. Since $\mathbf{g}_i$ and $\mathbf{s}_i$ are two orthogonal vectors that span the same subspace as $\mathbf{g}_i$ and $\mathbf{h}_i \times \mathbf{r}_i$, $\mathbf{f}_{bi}$ can be expressed as follows:

$$\mathbf{f}_{bi} = -\tau_i\,\mathbf{g}_i - \tau_i^{\perp}\,\mathbf{s}_i. \tag{19}$$

Equation (19) can be interpreted as the equilibrium of the forces applied on the upper part of the i^{th} limb. In fact, the two forces $\tau_i\,\mathbf{g}_i$ and $\tau_i^{\perp}\,\mathbf{s}_i$ are, respectively, the active axial and the passive shear forces applied through the actuated prismatic pair.

Replacing expression (19) for $\mathbf{f}_{bi}$ in (18), and taking into account that $\mathbf{g}_i \times (\mathbf{h}_i \times \mathbf{r}_i) = \mathbf{g}_i \times \mathbf{s}_i$ yields

$$\left(\frac{m_{hi}}{\mathbf{r}_i \cdot \mathbf{g}_i} - l_i\,\tau_i^{\perp} \right) (\mathbf{g}_i \times \mathbf{s}_i) = \mathbf{0}$$

which is satisfied if

$$m_{hi} = l_i\,\tau_i^{\perp}\,(\mathbf{r}_i \cdot \mathbf{g}_i). \tag{20}$$

Using (17), (20) can be rewritten as

$$m_{ri} = -l_i\,\tau_i^{\perp}\,(\mathbf{h}_i \cdot \mathbf{g}_i). \tag{21}$$

Regarding the end-effector equilibrium, the equilibrium of the forces is:

$$\mathbf{f}_{ext} = -\sum_{i=1}^{3}\mathbf{f}_{bi} = \sum_{i=1}^{3}\tau_i\mathbf{g}_i + \sum_{i=1}^{3}\tau_i^{\perp}\mathbf{s}_i \,, \tag{22}$$

and, taking the end-effector point P as reference point, the equilibrium of the moments is:

$$\mathbf{m}_{ext} = -\sum_{i=1}^{3} m_{hi}\mathbf{h}_i - \sum_{i=1}^{3}(\mathbf{b}_i - \mathbf{p})\times\mathbf{f}_{bi} \,. \tag{23}$$

The substitution of $\mathbf{f}_{bi}$, according to (19), and of m_{hi}, according to (20), into (23) yields

$$\mathbf{m}_{ext} = \sum_{i=1}^{3}\tau_i(\mathbf{b}_i - \mathbf{p})\times\mathbf{g}_i + \sum_{i=1}^{3}\tau_i^{\perp}[(\mathbf{b}_i - \mathbf{p})\times\mathbf{s}_i - l_i(\mathbf{r}_i\cdot\mathbf{g}_i)\mathbf{h}_i] \,. \tag{24}$$

Finally, Eqs. (22) and (24) can be rewritten in matrix form as follows:

$$\begin{pmatrix}\mathbf{f}_{ext}\\ \mathbf{m}_{ext}\end{pmatrix} = \begin{pmatrix}\mathbf{G}_{3\times3} & \mathbf{K}_{3\times3}\\ \mathbf{S}_{3\times3} & \mathbf{J}_{3\times3}\end{pmatrix}^{T}\begin{pmatrix}\boldsymbol{\tau}\\ \boldsymbol{\tau}^{\perp}\end{pmatrix} \tag{25}$$

where $\boldsymbol{\tau} = (\tau_1, \tau_2, \tau_3)^T$ is a vector collecting the signed magnitudes of the forces applied by the actuators in the prismatic pairs, and $\boldsymbol{\tau}^{\perp} = (\tau_1^{\perp}, \tau_2^{\perp}, \tau_3^{\perp})^T$.

Matrix relationship (25) is the input-output static relationship of the 3-nSPU. It is worth noting that, as expected, (11) and (25) satisfy the instantaneous power balance: $\mathbf{f}_{ext}\cdot\dot{\mathbf{p}} + \mathbf{m}_{ext}\cdot\boldsymbol{\omega} = \boldsymbol{\tau}\cdot\dot{\mathbf{l}}$.

3.3 Singularity Analysis: Singularities are manipulator configurations where the relationship (input-output instantaneous relationship) between the rates of the actuated-joint variables and the end-effector twist, ($\dot{\mathbf{p}}$, $\boldsymbol{\omega}$), fails [23–25]. Three types of singularities can be distinguished [23]: (I) singularities of the inverse kinematic problem, (II) singularities of the direct kinematic problem, and (III) singularities both of the inverse and of the direct kinematic problems. Type-I singularities occur when the actuated joint rates cannot be uniquely computed for an assigned end-effector twist. Vice versa, type-II singularities occur when the end-effector twist cannot be uniquely determined for assigned actuated joint rates.

For the 3-nSPU, the input-output instantaneous relationship is (11) where the actuated joint rates are collected in the vector $\dot{\mathbf{l}}$. This relationship highlights that the 3-nSPU has only three instantaneous dof. Therefore, its singularity analysis can be addressed by using the scheme proposed in [26].

Regarding type-I singularities, provided that the assigned twist, ($\dot{\mathbf{p}}$, $\boldsymbol{\omega}$), satisfies the last three equation of system (11), the inverse kinematic problem can be always solved[5].

Regarding type-II singularities, the equation of the singularity locus is

$$\det\begin{pmatrix}\mathbf{G}_{3\times3} & \mathbf{K}_{3\times3}\\ \mathbf{S}_{3\times3} & \mathbf{J}_{3\times3}\end{pmatrix} = 0 \tag{26}$$

The geometric interpretation of the above algebraic condition is not straightforward.

Nevertheless, the last three equations of system (11) allows the elimination of $\dot{\mathbf{p}}$ provided that $\det(\mathbf{S}_{3\times3}) = \mathbf{s}_1\cdot\mathbf{s}_2\times\mathbf{s}_3$ is different from zero. In this case, system (11) becomes

$$\dot{\mathbf{l}} = \mathbf{Q}\,\boldsymbol{\omega} \tag{27}$$

where $\mathbf{Q}$ is the 3×3 matrix ($\mathbf{K}_{3\times3} - \mathbf{G}_{3\times3}\,\mathbf{S}_{3\times3}^{-1}\,\mathbf{J}_{3\times3}$). Thus, the analytic expression of the singularity locus becomes

$$\det(\mathbf{Q}) = \mathbf{q}_1\cdot\mathbf{q}_2\times\mathbf{q}_3 \tag{28}$$

where the vectors $\mathbf{q}_i$, for i = 1, 2, 3, are the column vectors of matrix $\mathbf{Q}$. In conclusion, if the mixed product $\mathbf{s}_1\cdot\mathbf{s}_2\times\mathbf{s}_3$ is different from zero (i.e., the three vectors $\mathbf{s}_i$, for i = 1, 2, 3, are neither coplanar nor null vectors), the type-II singularities are geometrically identified by either the coplanarity of the three vectors $\mathbf{q}_i$, for i = 1, 2, 3, or by the fact that at least one of the $\mathbf{q}_i$ vectors is a null vector.

If the mixed product $\mathbf{s}_1\cdot\mathbf{s}_2\times\mathbf{s}_3$ is zero, the determinant of the whole 6×6 matrix appearing in (26) must be considered, and geometric interpretations of (26) are much more difficult to provide.

The zeroing of $\mathbf{s}_1\cdot\mathbf{s}_2\times\mathbf{s}_3$ can be geometrically identified since it occurs when either (*a*) at least one of the $\mathbf{s}_i$ vectors is a null vector, or (*b*) the three $\mathbf{s}_i$ vectors are coplanar. Vector $\mathbf{s}_i$ (see definition (10)) is related to the configuration of the i^{th} limb, and it is the component of $\mathbf{h}_i\times\mathbf{r}_i$ perpendicular to $\mathbf{g}_i$ (i.e., to the limb axis).

As a consequence, condition (*a*) occurs when, in at least one limb, either (*a*.1) the two unit vectors $\mathbf{h}_i$ and $\mathbf{r}_i$ are parallel (i.e., when, in a limb, the revolute pair axes in the U joint are both parallel to the plane defined by the roller axis and the sphere center in the nS pair), or (*a*.2) the limb axis is the intersection line between the plane, defined by the roller axis and the sphere center in the nS pair, and the plane, defined by the revolute pair axes of the U joint. Condition (*a*.2) is forbidden in practice by the actual sizes of joints and links. Regarding condition (*a*.1), a very special case occurs when $\mathbf{h}_i$ and $\mathbf{r}_i$ are parallel in all the limbs. This occurrence makes the matrix $\mathbf{S}_{3\times3}$ a null matrix and allows the determinant at the left-hand side of (26) to be factorized as $\det(\mathbf{G}_{3\times3})\,\det(\mathbf{J}_{3\times3})$ where $\det(\mathbf{G}_{3\times3})$ is equal to $\mathbf{g}_1\cdot\mathbf{g}_2\times\mathbf{g}_3$, whereas, in this case, $\det(\mathbf{J}_{3\times3})$ is equal to $-l_1l_2l_3\,(\mathbf{r}_1\cdot\mathbf{g}_1)\,(\mathbf{r}_2\cdot\mathbf{g}_2)\,(\mathbf{r}_3\cdot\mathbf{g}_3)\,\mathbf{h}_1\cdot\mathbf{h}_2\times\mathbf{h}_3$. Thus, in this case, a type-II singularity occurs when either the limb axes are all parallel to a unique plane, or the $\mathbf{h}_i$ vectors are coplanar, or, finally, in at least one limb, the limb axis lies on the plane defined by the roller axis and the sphere center of the nS pair. Moreover, it is worth noting that, in this case, the end effector performs an instantaneous translation, if neither $\det(\mathbf{G}_{3\times3})$ nor $\det(\mathbf{J}_{3\times3})$ are equal to zero (i.e., out of singularity).

Regarding condition (*b*) (i.e., the coplanarity of the $\mathbf{s}_i$ vectors), it occurs when the limb axes are all parallel, and in other configurations more difficult to visualize.

3.4 Local and Global Controllability: Each end-effector configuration (pose) can be modeled as a point in $R^3\times SO(3)$

[5] System (11) does not model the mobility limitations due to the physical constitution of the real joints, and to the real sizes of the links. Such limitations bound the workspace and, when correctly modeled, yield type-I singularities.

which is locally diffeomorphic to R^6 equipped with a proper set of local coordinates: $\mathbf{x} \equiv (\mathbf{p}^T, \boldsymbol{\eta}^T)^T$ where $\boldsymbol{\eta}$ is a three-dimensional vector collecting the values of the three orientation parameters chosen to locate end-effector's orientation.

By using the orientation parameters' rates, $\dot{\boldsymbol{\eta}}$, the end-effector's angular velocity, $\boldsymbol{\omega}$, can be expressed as:

$$\boldsymbol{\omega} = \mathbf{H}_{3\times3}\ \dot{\boldsymbol{\eta}} \tag{29}.$$

Relationship (29) allows system (11) to be rewritten in the form

$$\dot{\mathbf{x}} = \mathbf{V}_{6x6}\begin{pmatrix} \dot{\mathbf{i}} \\ \mathbf{0}_{3x1} \end{pmatrix} \tag{30}$$

with

$$\mathbf{V}_{6x6} \triangleq (\mathbf{v}_1,\mathbf{v}_2,\mathbf{v}_3,\mathbf{v}_4,\mathbf{v}_5,\mathbf{v}_6) = \begin{pmatrix} \mathbf{1}_{3\times3} & \mathbf{0}_{3\times3} \\ \mathbf{0}_{3\times3} & \mathbf{H}^{-1}_{3x3} \end{pmatrix}\begin{pmatrix} \mathbf{G}_{3\times3} & \mathbf{K}_{3\times3} \\ \mathbf{S}_{3\times3} & \mathbf{J}_{3\times3} \end{pmatrix}^{-1} \tag{31}$$

where $\mathbf{v}_i$ is the i-th 6-dimensional column vector of matrix $\mathbf{V}_{6x6}$. The vectors $\mathbf{v}_i$ depend only on $\mathbf{x}$; so, they are vector fields defined on end-effector's configuration space.

Definition (31) allows (30) to be further simplified as follows:

$$\dot{\mathbf{x}} = \mathbf{v}_1 \dot{l}_1 + \mathbf{v}_2 \dot{l}_2 + \mathbf{v}_3 \dot{l}_3 \tag{32}.$$

Relationship (32) states that, in the neighborhood of a generic configuration, $\mathbf{x}_0$, all the configurations, $\mathbf{x}$, reachable without maneuvering (i.e., without a sequence of coordinated actions of the actuators) are so located that $(\mathbf{x}-\mathbf{x}_0) \in \text{Span}(\mathbf{v}_1, \mathbf{v}_2, \mathbf{v}_3)$.

(32) is the relationship to be considered for discussing end-effector's ability to reach any configuration in the neighborhood of a generic configuration, $\mathbf{x}_0$ [27, 28]. The presence of non-holonomic constraints in the 3-nSPU manipulator might allow all neighboring configurations be reachable possibly by maneuvering. If this happened, the system would be "locally controllable" [27] at the configuration $\mathbf{x}_0$.

It can be shown (see [28] pp 323-324) that, if a system, satisfying (32) and at the configuration $\mathbf{x}_0$, first follows $\mathbf{v}_i$, $i\in\{1,2,3\}$, for a small time ε, then follows $\mathbf{v}_j$, $j\in\{1,2,3 \mid j\neq i\}$, for the same time ε, then $-\mathbf{v}_i$ for ε, and finally $-\mathbf{v}_j$ for ε, it will reach the following configuration of x_0's neighborhood:

$$\lim_{\varepsilon\to0} \mathbf{x}(4\varepsilon) = \mathbf{x}_0 + \varepsilon^2[\mathbf{v}_i,\mathbf{v}_j]_{\mathbf{x}=\mathbf{x}_0} \tag{33}$$

where $[\mathbf{v}_i, \mathbf{v}_j]$ is the 6-dimensional vector field named Lie product of $\mathbf{v}_i$ and $\mathbf{v}_j$, defined as follows

$$[\mathbf{v}_i,\mathbf{v}_j] = \frac{\partial \mathbf{v}_j}{\partial \mathbf{x}}\mathbf{v}_i - \frac{\partial \mathbf{v}_i}{\partial \mathbf{x}}\mathbf{v}_j \tag{34},$$

and the trailing subscript, $\mathbf{x} = \mathbf{x}_0$, indicates the point the two vector fields, $\mathbf{v}_i$ and $\mathbf{v}_j$, are evaluated at.

By reiterating the same reasoning (first, on pairs of vector fields of type $\mathbf{v}_i$ and $[\mathbf{v}_j, \mathbf{v}_k]$, $i,j,k\in\{1,2,3 \mid i\neq j\neq k\}$, and, successively, on pairs of vector fields belonging to the set which collects all the vector fields that, in the previous iterations, were demonstrated to point from $\mathbf{x}_0$ toward reachable configurations), it can be demonstrated that all the vector fields obtained through Lie products of any degree of elements of the set $\{\mathbf{v}_1, \mathbf{v}_2, \mathbf{v}_3\}$ point toward configurations that are reachable by maneuvering from $\mathbf{x}_0$ [27]. In other word, for any reachable configuration, say $\mathbf{x}$, the vector $(\mathbf{x}-\mathbf{x}_0)$ belongs to the Lie algebra[6] of $\{\mathbf{v}_1, \mathbf{v}_2, \mathbf{v}_3\}$.

In our case, demonstrating that the dimension of the linear space $\text{Span}(\mathbf{v}_1, \mathbf{v}_2, \mathbf{v}_3, [\mathbf{v}_1, \mathbf{v}_2], [\mathbf{v}_1, \mathbf{v}_3], [\mathbf{v}_1, \mathbf{v}_2])$ is six[7] is sufficient for concluding that the manipulator is locally controllable at a given configuration since end-effector's configuration space is 6-dimensional (Chow's theorem [28]). Moreover, showing that the set of configurations where the system is locally controllable is a simply connected region is sufficient to demonstrate the existence of finite regions of end-effector's configuration space where, for any two configurations belonging to that region, at least one path exists, which the system can follows, for moving from one configuration to the other (i.e., the system is "globally controllable" in that region).

According to the above discussion, the configurations where the local controllability of our manipulator is not guaranteed are the geometric locus of the roots of the following equation

$$\det(\mathbf{L}_{6\times6}) = 0 \tag{35}$$

where

$$\mathbf{L}_{6\times6} \triangleq (\mathbf{v}_1, \mathbf{v}_2, \mathbf{v}_3, [\mathbf{v}_1,\mathbf{v}_2], [\mathbf{v}_1,\mathbf{v}_3], [\mathbf{v}_2,\mathbf{v}_3]) \tag{36}.$$

The locus of the roots of (35) is in general a 5-dimensional variety; thus, a finite region where our manipulator is globally controllable in general exists. This statement will be verified through the numerical example reported below.

3.5 Numerical Example: With reference to the notation defined in the Figs. 5 and 6, a 3-nSPU is considered where the points A_i (B_i) for i=1,2,3 are at the vertices of an equilateral triangle fixed to the frame (to the end effector). The Cartesian reference system fixed to the frame (to the end effector) has the origin O (P) at the centroid of the equilateral triangle, z axis perpendicular to the plane of the triangle, x axis passing through A_3 (B_3) with direction from A_3 (B_3) toward O (P), and y axis accordingly chosen. In an arbitrary unit of length (aul), the distance of the triangle vertices A_i (B_i) from its centroid is 39.7 aul (11.76 aul). In the same unit, the geometry of the frame and of the end effector are defined by the following data (the vector without any leading superscript are measured in the frame reference, whereas the vectors with the leading superscript $^e(\cdot)$ are measured in the end-effector reference): $\mathbf{a}_1=(19.85,\ -34.3812,\ 0)^T$, $\mathbf{a}_2=(19.85,\ 34.3812,\ 0)^T$, $\mathbf{a}_3=(39.7,\ 0,\ 0)^T$, $\mathbf{r}_1=(0.7887,\ -0.2113,\ 0.5774)^T$, $\mathbf{r}_2=(-0.2113,\ 0.7887,\ 0.5774)^T$, $\mathbf{r}_3=(-0.5774,\ 0.5774,\ 0.5774)^T$, $^e(\mathbf{b}_1-\mathbf{p})=(5.88,\ -10.1845,\ 0)^T$, $^e(\mathbf{b}_2-\mathbf{p})=(5.88,\ 10.1845,\ 0)^T$, $^e(\mathbf{b}_3-\mathbf{p})=(11.76,\ 0,\ 0)^T$, $^e\mathbf{w}_{41}=(0.3536,\ -0.6124,\ 0.7071)^T$, $^e\mathbf{w}_{42}=(0.3536,\ 0.6124,\ 0.7071)^T$, $^e\mathbf{w}_{43}=(-0.7071,\ 0,\ 0.7071)^T$.

With this manipulator geometry, the singularity locus defined by Eq. (26) and the root locus of Eq. (35) have been computed for a fixed orientation of the end effector with respect to the frame.

[6] The "Lie algebra" of a set of vector fields is the linear span of all Lie products, of all degrees, of vector fields belonging to that set [27].

[7] It is worth noting that, if the dimension of $\text{Span}(\mathbf{v}_1, \mathbf{v}_2, \mathbf{v}_3, [\mathbf{v}_1,\mathbf{v}_2], [\mathbf{v}_1,\mathbf{v}_3], [\mathbf{v}_2,\mathbf{v}_3])$ is six, all the Lie products of any degree in $\{\mathbf{v}_1, \mathbf{v}_2, \mathbf{v}_3\}$ must belong to $\text{Span}(\mathbf{v}_1, \mathbf{v}_2, \mathbf{v}_3, [\mathbf{v}_1,\mathbf{v}_2], [\mathbf{v}_1,\mathbf{v}_3], [\mathbf{v}_2,\mathbf{v}_3])$; thus, all the reachable configurations, $\mathbf{x}$, satisfy the condition $(\mathbf{x}-\mathbf{x}_0)\in \text{Span}(\mathbf{v}_1, \mathbf{v}_2, \mathbf{v}_3, [\mathbf{v}_1,\mathbf{v}_2], [\mathbf{v}_1,\mathbf{v}_3], [\mathbf{v}_2,\mathbf{v}_3])$.

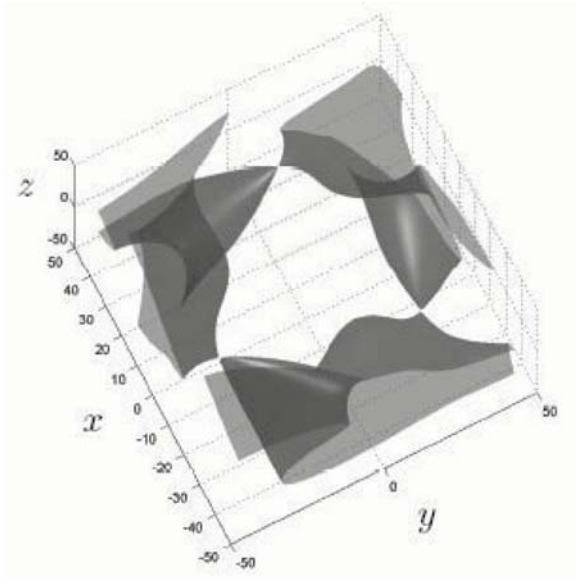

Figure 7. Singularity locus [Eq. (26)] for the 3-nSPU geometry of the numerical example, and end-effector orientation fixed to XZX Euler angles' values (0, 1, 0) radians: (a) 3D view, (b) top view

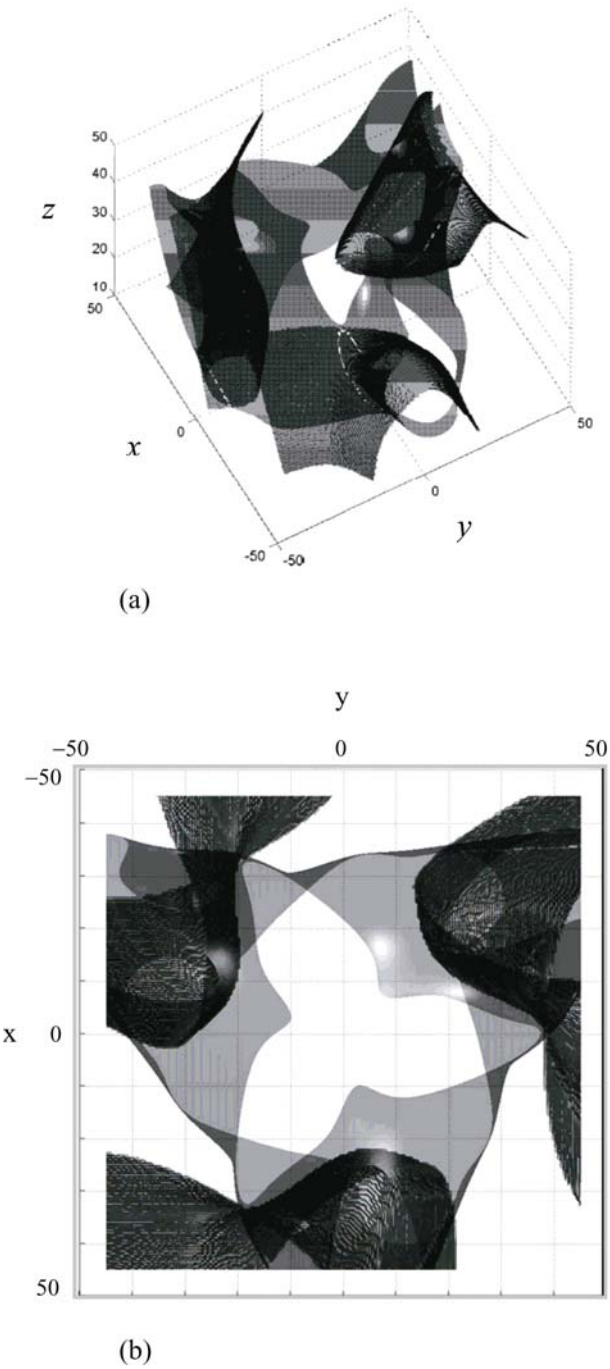

Figure 8. Locus of the Eq. (35) roots for the 3-nSPU geometry of the numerical example, and end-effector orientation fixed to XZX Euler angles' values (0, 1, 0) radians: (a) 3D view, (b) top view

The results of these two computations are shown in the Figs. 7 and 8, respectively. By comparing the singularity locus (Fig. 7) and the root locus of Eq. (35) (Fig. 8), a wide free-from-singularity region that is globally controllable can be easily identified.

4 Conclusions

If a number of non-holonomic spherical pairs replaces as many spherical pairs in a manipulator, the same number of actuators can be eliminated. The resulting manipulator will keep

the same workspace of the generating manipulator, but it will be under-actuated.

This technique for generating under-actuated manipulators can be applied to fully-parallel manipulators, where many spherical pairs are present, and the elimination of an actuator in an UPS limb can be accompanied with the elimination of the whole UPS limb.

Through this pair substitution, an under-actuated manipulator, previously proposed by one of the authors, has been generated from an inversion of the 6-3 FPM. The kinetostatic analysis of this manipulator has been reconsidered to obtain a simple and compact formulation. This reformulated analysis can be used both in the design of the under-actuated manipulator, and in its control. Further works on this manipulator will present an exhaustive singularity analysis, and will provide design criteria for increasing its useful workspace.

Acknowledgements

This work has been partially supported by the Spanish Ministry of Education and Science, under the I+D project DPI2007-60858, and by Italian MIUR funds. We also like to thank our colleagues Patricia Ben-Horin, from Technion, Israel, and Krzysztof Tchon, from Wroclaw University of Technology, Poland, for their helpful comments.

References

[1] Shammas, E.A., Choset, H., and Rizzi, A.A., 2007, "Towards a Unified Approach to Motion Planning for Dynamic Underactuated Mechanical Systems with Non-holonomic Constraints," *The International Journal of Robotics Research*, Vol. 26, No. 10, October 2007, pp. 1075–1124.

[2] Hussein, I.I., and Bloch, A.M., 2008, "Optimal Control of Underactuated Nonholonomic Mechanical Systems," *IEEE Transactions On Automatic Control*, Vol. 53, No. 3, April 2008, pp. 668-682

[3] De Luca, A., Oriolo, G., and Robuffo-Giordano, P., 2007, "Image-based visual servoing schemes for nonholonomic mobile manipulators," *Robotica*, Vol. 25 (2007), pp. 131–145

[4] Duleba, I., and Khefifi, W., 2007, "Velocity space approach to motion planning of nonholonomic systems," *Robotica*, Vol. 25 (2007), pp. 359–366

[5] Angeles, J., 2003, "Fundamentals of robotic mechanical systems," Springer-Verlag, New York, NY.

[6] O'Reilly, O. M., 2008, "Intermediate dynamics for engineers," Cambridge University Press, New York, NY.

[7] Stammers, C. W., Prest, P. H., and Mobley, C. G., 1992, "A friction drive robot wrist: electronic and control requirements," Mechatronics, Vol. 2, No 4, pp. 391 – 401.

[8] Peshkin, M., Colgate, J. E., and Moore, C., 1996, "Passive robots and haptic displays based on nonholonomic elements," Proc. of the 1996 IEEE Int. Conf. on Robotics and Automation, pp. 551 – 556.

[9] Nakamura, Y., Chung, W., and Sørdalen, O. J., 2001, "Design and control of the nonholonomic manipulator," IEEE Trans. on Robotics and Automation, Vol 17, No. 1, pp. 48 – 59.

[10] Ben-Horin, P., and Thomas, F., 2008, "A nonholonomic 3-motor parallel robot," In: Advances in Robot Kinematics, J. Lenarcic and P. Wenger, eds. Springer Verlag.

[11] Hennessey, M. P., 2006, "Visualizing the motion of a unicycle on a sphere," Int. J. of Modelling and Simulation, Vol. 26, No. 1, pp. 69 – 79.

[12] Lu, Y., Shi, Y., Li, S.-H., and Tian, X.-B., 2008, "Synthesis and Analysis of Kinematics/Statics of a Novel 2SPS+SPR+SP Parallel Manipulator," *Journal of Mechanical Design*, September 2008, Vol. 130, pp. 092302-1/8

[13] Tahmasebi, F., 2007, "Kinematics of a New High-Precision Three-Degree-of-Freedom Parallel Manipulator," *Journal of Mechanical Design*, March 2007, Vol. 129, pp. 320-325.

[14] Gallardo-Alvarado, J., Orozco-Mendoza, H., and Maeda-Sánchez, A., 2007, "Acceleration and singularity analyses of a parallel manipulator with a particular topology," *Meccanica*, Vol. 42 (2007), pp. 223–238.

[15] Innocenti, C., and Parenti-Castelli, V., 1994, "Exhaustive enumeration of fully-parallel kinematic chains," Proc. of the 1994 ASME Int. Winter Annual Meeting, Vol. 55-2 of DSC, pp. 1135 – 1141.

[16] Stewart, D., 1965, "A platform with six degrees of freedom," In Proc. of the Institution of Mechanical Engineers, Vol. 180-5, pp. 371 – 378.

[17] Innocenti, C., and Parenti-Castelli, V., 1990, "Direct position analysis of the Stewart platform mechanism," Mechanism and Machine Theory, Vol. 25, No. 6, pp. 611 – 621.

[18] Parenti-Castelli, V., and Di Gregorio, R., 1996, "Closed-form solution of the direct kinematics of the 6-3 type Stewart platform using one extra sensor," Meccanica, Vol. 31, pp. 705 – 711.

[19] Ji, C.-Y., Chen, T.-C., and Lee, Y.-L., 2007, "Investigation of Kinematic Analysis and Applications for a 3-RRPS Parallel Manipulator," *Journal of the Chinese Society of Mechanical Engineers*, Vol.28, No.6, pp.623-632 (2007)

[20] Sokolov, A., and Xirouchakis, P., 2007, "Dynamics analysis of a 3-DOF parallel manipulator with R–P–S joint structure," *Mechanism and Machine Theory*, Vol. 42 (2007), pp. 541–557

[21] Farhat, N., Mata, V., Page, À., and Valero, F., 2008, "Identification of dynamic parameters of a 3-DOF RPS parallel manipulator," *Mechanism and Machine Theory*, Vol. 43 (2008), pp. 1–17

[22] Rao, N.M., and Rao, K. M., 2009, "Dimensional synthesis of a spatial 3-RPS parallel manipulator for a prescribed range of motion of spherical joints," *Mechanism and Machine Theory*, Vol. 44 (2009), pp. 477–486

[23] Gosselin, C. M., and Angeles, J., 1990, "Singularity analysis of closed-loop kinematic chain," IEEE Transactions on Robotics and Automation, Vol. 6, No. 3, pp. 281 – 290.

[24] Ma, O., and Angeles, J., 1991, "Architecture singularities of platform manipulators," Proc. of the 1991 IEEE Int. Conf. on Robotics and Automation, pp. 1542 – 1547.

[25] Zlatanov, D., Fenton, R. G., and Benabib, B., 1995, "A unifying framework for classification and interpretation of mechanism singularities" ASME Journal of Mechanical Design, Vol. 117, No. 4, pp. 566 – 572.

[26] Di Gregorio, R., 2008, "An exhaustive scheme for the singularity analysis of three-dof parallel manipulators," Proc. of the 17th International Workshop on Robotics in Alpe-Adria-Danube Region, Ancona, Italy.

[27] Choset, H., Lynch, K.M., Hutchinson, S., Kantor, G., Burgard, W., Kavraki, L.E., and Thrun, S., 2005, "Principles of Robot Motion: Theory, Algorithms, and Implementations," MIT Press, Boston.

[28] Murray, R.M., Li, Z., and Sastry, S.S., 1994, "A Mathematical introduction to robotic manipulation," CRC Press, Boca Raton.